All Sciences Proceedings
http://as-proceeding.com/

2nd International Conference on Engineering, Natural and Social Sciences

April 4-6, 2023 : Konya, Turkey

https://www.icensos.com/

Fractional Order Sliding Mode Controller for Heading and Heave Control of Quadcopter

Abdul Haseeb*, Ahsan Ali [2] and Inam ul Hasan [3]

[1]Department of Electrical Engineering, University of Engineering and Technology Taxila, Pakistan
[2]Department of Electrical Engineering, University of Engineering and Technology Taxila, Pakistan
[3]Department of Electrical Engineering, University of Engineering and Technology Taxila, Pakistan

*Abdul.haseeb@students.uettaxila.edu.pk Email of the corresponding author

Abstract – In this paper a fractional order sliding mode control (FO-SMC) based approach is proposed to a six-degree of freedom (6-DOF) quadcopter for the control of heading and heave. We begin by describing the mathematical model of a quadcopter. Afterward, a nonlinear controller is designed to maintain the quadcopter's heading and heave while tracking the desired outputs. FOSMC has been shown to eliminate heading and heave tracking errors, even when external disturbances occur. A simulation test is performed to verify the robustness of the proposed controller.

Keywords – Multi-Rotor Unmanned Aerial Vehicle (MUAV), Unmanned Aerial Vehicle (UAV), Fractional Order Sliding Mode Controller (FO-SMC), Under-Actuated Systems (UAS), Degrees Of Freedom (DOF).

I. INTRODUCTION

From the last few years, the control of Unmanned Aerial Vehicles has all progressed significantly. The goal of this effort is to create a fractional order sliding mode quadrotor controller. There are discrepancies between the actual plant and the mathematical model used for controller design when a control problem is formulated. The fractional sliding mode controller tries to correct this mismatch. A Simulink model of six degrees of freedom is used to show the suggested approach. For the controller design of other MUAV systems as well as other nonlinear under-actuated systems, the suggested methodologies give effective guidance. The efficiency of linearized dynamics-based control schemes outside of the operating region is a critical topic to address. Linearizing the system at operational points and then applying linear control strategies is a common method of controlling the UAV. The disadvantage of this strategy is that when used outside of the working region, the proposed controller based on linear system dynamic does not perform well. This issue can be resolved by using a linear parameters variable system model.

In [3], the scholars proposed the research on quadcopter control by using the adaptive compensation technique. By using this their system can be able to detect the fault and recover it may as possible. Yaw, pitch, and roll into consideration. The change of angle is taken from -6° to +6°. A simple adaptive control by taking the linearized model along with the fuzzy logic feedforward compensator is used [4]. The system can optimize the parameters which are involved in the controller if some disturbance is injected into the system and reconfiguration control capability involved. Also, in [5] researchers propose an adaptive backstepping control, focus on the 1 degree of freedom that is the thrust force and the other three in angular velocities. The model and control of the coaxial octo rotor are presented [6]. First group that models the eight rotors unmanned aerial vehicle (UAV).

The robust controller is achieved by the backstepping sliding mode controller (BSMC) with an adaptive radial basis function neural network

(RBNN). In [7] worked on designing and implementing the controller of eight rotor UAVs, they performs several experiments but their system is only attitude controller-based by using the proportional integral derivative (PID) controller. During running if one of the motors is stopped working. Then for it, a recovery algorithm is implemented to diagnose it and overcome the loss. At this time multirotor is allowed to complete the flight [8]. An adaptive technique-based controller of the quadcopter is used to achieve the robustness by applying the ASMC (adaptive sliding mode controller) with some uncertainties. They developed an algorithm based on the Lyapunov function and compared their result with the previous controller and showed the stability of the proposed model [9]. In [10] the nature of team work, is fault detection and recovery algorithm for the eight rotor UAVs with second-order sliding mode observer with unknown input uncertainties. Further the failure of motors during flight the offline control mixing strategy is involved. In which system can be adopted the input by built in command and gives the output according to the given situation. Performing the experimental results, authors achieved a good response if two motors are failed during the flight [11]. On linearized model scholars performed hover situation of quadcopter with the H-infinity mixed-sensitivity controller. Control of attitude of the quadcopter by using the μ-synthesis controller. This is the next step of the H-infinity controller by doing the DK iterations. Their research concluded that applied controller is good for robust stability and robust performance [12]-[13].

II. PRELIMINARIES

A. *Dynamics of Quadcopter*

The quadrotor is the most prevalent UAV variant for several purposes. A quadrotor is made up of four rotors those are equally distanced "x" from the pivot point and installed at the extremities of a cross airframe design as shown in Figure 1. The four electric motors cause the thrust "T" and speed "ω" of the rotors. Necessary thrust required to lift the quadcopter upward. Each rotor rotates in the opposite direction of the rotors next to it. Rotors 1 and 3 rotate in the opposite direction i.e., clockwise, while rotors 2 and 4 rotate in the opposite direction i.e., anti-clockwise. The subscript "B" shows the body frame representation.

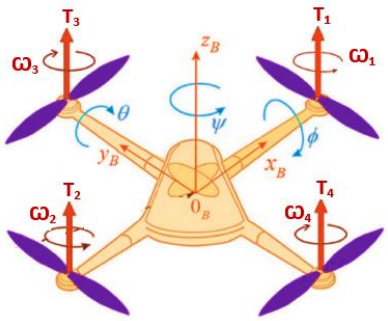

Fig. 1 Layout of Quadcopter

B. *Quadcopter Equation of Motion*

The total thrust is given by,

$$T_i = k_F \omega_i \tag{1}$$

Where "T" denotes the total thrust applied on the quadcopter which moves it upward. Where i = 1, 2, 3 and 4, and k_F is the force coefficient, ω_i denotes the speed of the rotors.

$$M_i = k_M \omega_i \tag{1}$$

where k_M is the moment coefficient.

By expanding the above equations following is obtained,

$$\vec{T} = \overrightarrow{T_1} + \overrightarrow{T_2} + \overrightarrow{T_3} + \overrightarrow{T_3} - \overrightarrow{mgh} \tag{3}$$

And,

$$\vec{M} = r_1\overrightarrow{T_1} + r_2\overrightarrow{T_2} + r_3\overrightarrow{T_3} + r_4\overrightarrow{T_4} + \overrightarrow{M_1} + \overrightarrow{M_2} + \overrightarrow{M_3} + \overrightarrow{M_4} \tag{4}$$

Equation 3 and 4 shows the net force and the net moment. If we combine these equations with the Newton-Euler equations, we get the following set of equations.

$$m\ddot{r} = \begin{bmatrix} 0 \\ 0 \\ -mg \end{bmatrix} + R \begin{bmatrix} 0 \\ 0 \\ T_1 + T_2 + T_3 + T_4 \end{bmatrix} \tag{5}$$

$$J \begin{bmatrix} \dot{p} \\ \dot{q} \\ \dot{r} \end{bmatrix} = \begin{bmatrix} x(T_2 - T_4) \\ x(T_3 - T_1) \\ T_1 - T_2 + T_3 - T_4 \end{bmatrix} - \begin{bmatrix} p \\ q \\ r \end{bmatrix} \times J \begin{bmatrix} p \\ q \\ r \end{bmatrix} \tag{6}$$

The matrix R is rotating thrust vector, quadrotor's inertia with respect to body frame. The quadcopter will experience a force in the z direction if all the rotor speeds are equal. Depending on the strength of the force concerning gravity, the quadcopter will either go up, hover, or fall. Pitch, roll, and yaw motion are caused by the moments acting on the quadcopter. Due to the difference in thrust generated by motors 2 and 4, the pitching moment M occurs. Due to the difference in thrust generated by motors 1 and 3, the rolling moment M occurs. The drag force that opposes the rotation of all the propellers causes the yawing moment M.

C. Mathematical Modelling

UAVs are a category of underactuated nonlinear mechanical systems, which are traditionally challenging to manage because they have fewer control inputs than degrees of freedom [16]. There have so far been two primary methods employed for MUAV modelling. The goal is to create a dynamic model of the MUAV that exhibits strong coupling and nonlinearities between various modules. Therefore, modelling is a crucial step in creating flight controllers for UAVs. As seen in Figure 2, a dynamical model of the MUAV system is a collection of mathematical equations that link the system's inputs and outputs.

It may be broken down into four modules: 6-DOF rigid body dynamics, actuator dynamics, rotor dynamics, and force and moment production mechanism [17]. MUAV is treated as a rigid body in Cartesian space with a system for producing force and torque vectors when designing control for it. Generally, Newton–Euler equations of motion are used to describe the dynamics of rigid-body, or Euler-Lagrange equations for energy-oriented approaches. The body frame or the inertial frame can be used to express the resultant equations of motion, having different model structures and parameters. Most of the researchers have relayed on these techniques for modelling and control of MUAV, that can be seen in [18-19].

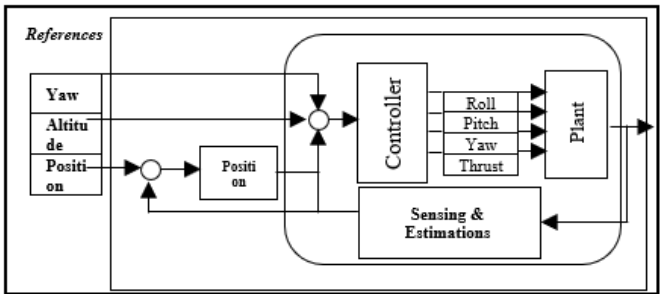

Fig. 2 Main Components of a Typical UAV Dynamical Model

D. Kinematic Modelling

The coordinate systems utilized in the dynamic equations' derivations are shown in Figure 3. Let r^I indicate where the quadrotor's center of mass is in a frame of global coordinates.

$$r^I = [x^I \quad y^I \quad z^I]^T \tag{7}$$

The quadrotor's speed about the global coordinate frame expressed in the global frame is indicated by the symbol v^I.

$$v^I = \dot{r}^I = [\dot{x}^I \quad \dot{y}^I \quad \dot{z}^I]^T \tag{8}$$

The quadrotor's centre of mass serves as the origin of a body-frame coordinate system with the coordinates x^B, y^B, and z^B. In Euler-angles, the quadrotor's orientation η is described (yaw, pitch, roll).

$$\eta = [\psi \quad \theta \quad \phi]^T \tag{9}$$

yaw ψ = global z-axis rotation first
pitch θ = new y-axis rotation
roll ϕ = new x-axis rotation

The matrix W^{-1} transforms the body-angular rates about local x-y-z-axes to Euler-rates.

$$\Omega = (p, q, r)^T \tag{10}$$

$$\dot{\eta} = \left[\dot{\psi} \quad \dot{\theta} \quad \dot{\phi}\right]^T \tag{11}$$

$$W^{-1} = \begin{bmatrix} 0 & \frac{\sin(\phi)}{\cos(\theta)} & \frac{\cos(\phi)}{\cos(\theta)} \\ 0 & \cos(\phi) & -\sin(\phi) \\ 1 & \sin(\phi)\tan(\theta) & \cos(\phi)\tan(\theta) \end{bmatrix} \tag{12}$$

E. Dynamical Modelling

The simplest dynamic model to describe the quadrotor's dynamics with its full 6-DOF. Let,

T^B = Total thrust generated by the rotors expressed in the body frame
τ_{yaw} *= total torque about the* z^B*-axis*
τ_{pitch} *= total torque about the* y^B*-axis*
τ_{roll} *=total torque about the* x^B*-axis*
J= quadrotor's inertia w.r.t body frame

Now according to Newtons second law
Net Force = mass × acceleration

$$D_B^I(\eta)T^B = m(\dot{v}^I - G^I) \tag{13}$$

$$\dot{v}^I = G^I + D_B^I(\eta)\frac{T^B}{m} \tag{14}$$

With D_B^I denotes the transformation matrix from body-frame axes to the inertial frame axes,

$$D_B^I(\eta) = D_\psi D_\theta D_\phi \tag{15}$$

$$D_\psi = \begin{bmatrix} cos(\psi) & -sin(\psi) & 0 \\ -sin(\psi) & cos(\psi) & 0 \\ 0 & 0 & 1 \end{bmatrix} \tag{16}$$

$$D_\theta = \begin{bmatrix} cos(\theta) & 0 & cos(\theta) \\ 0 & 1 & 0 \\ -sin(\theta) & 0 & cos(\theta) \end{bmatrix} \tag{17}$$

$$D_\phi = \begin{bmatrix} 1 & 0 & 0 \\ 0 & cos(\phi) & -sin(\phi) \\ 0 & sin(\phi) & cos(\phi) \end{bmatrix} \tag{18}$$

Also, Net Moment = Inertia × angular acceleration

$$\begin{bmatrix} \tau_{roll} \\ \tau_{pitch} \\ \tau_{yaw} \end{bmatrix} = J\dot{\Omega} + \Omega \times J\Omega \quad (19)$$

$$J\dot{\Omega} = \begin{bmatrix} \tau_{roll} \\ \tau_{pitch} \\ \tau_{yaw} \end{bmatrix} - \Omega \times J\Omega \quad (20)$$

$$\dot{\eta} = W^{-1}\Omega \quad (21)$$

$$\begin{bmatrix} \dot{\psi} \\ \dot{\theta} \\ \dot{\phi} \end{bmatrix} = W^{-1} \begin{bmatrix} p \\ q \\ r \end{bmatrix} \quad (22)$$

As a result of having more degrees of freedom than real control inputs (the four motor speeds w_i), this system is underactuated. The transformation of motor speeds w_i to $\begin{bmatrix} T^B & \tau_{roll} & \tau_{pitch} & \tau_{yaw} \end{bmatrix}^T$ is given by:

$T = \alpha_T(\omega_0^2 + \omega_1^2 + \omega_2^2 + \omega_3^2)$.

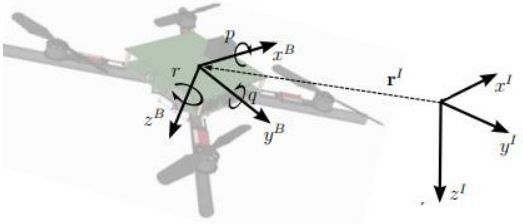

Fig. 3 Coordinate Frames [29]

The quadcopter UAV dynamics in 6-DOF are provided as follows [30],

$$\ddot{x} = (cos\phi\ sin\theta\ cos\psi + sin\phi\ sin\psi)\frac{u_1}{m} \quad (23)$$

$$\ddot{y} = (cos\phi\ sin\theta\ cos\psi - sin\phi\ sin\psi)\frac{u_1}{m} \quad (24)$$

$$\ddot{z} = -g + (cos\phi\ cos\theta)\frac{u_1}{m} \quad (25)$$

$$\ddot{\phi} = a_1\dot{\theta}\dot{\psi} + a_2\dot{\theta}\Omega_d + \frac{1}{I_x}u_2 \quad (26)$$

$$\ddot{\theta} = a_3\dot{\phi}\dot{\psi} + a_4\dot{\phi}\Omega_d + \frac{1}{I_y}u_3 \quad (27)$$

$$\ddot{\psi} = a_5\dot{\phi}\dot{\theta} + \frac{1}{I_z}u_4 \quad (28)$$

Where,

$$a_1 = \frac{I_y - I_z}{I_x}, a_2 = \frac{J_r}{I_x}, a_3 = \frac{I_z - I_x}{I_y}, a_4 = \frac{J_r}{I_y},\ and\ \ a_5 = \frac{I_x - I_y}{I_z} \quad (29)$$

Jr is for rotor inertia, and I_x, I_y, and I_z represents the x, y, and z-axis inertia, respectively. Quadrotor's parameters values for these constants are shown in Table 1.

And (u_1, u_2, u_3, u_4) are the control inputs given as follows.

Table 1. Quadcopter's Parameters

Name	Parameter	Value
Mass	m	0.063 kg
Inertia x-axis	Ix	0.0000582857 kgm^2
Inertia y-axis	Iy	0.0000716914 kgm^2
Inertia z-axis	Iz	0.0001 kgm^2
Thrust coefficient	b	4.719990366910910e-08 Ns^2
Rotor Inertia	Jr	1.0209375e-07 kgm^2
Arm Length	d	0.1080 m

$$u_1 = \mathrm{b}(\Omega_1^2 + \Omega_2^2 + \Omega_3^2 + \Omega_4^2) \quad (30)$$

$$u_2 = \mathrm{b}(\Omega_4^2 - \Omega_2^2) \quad (31)$$

$$u_3 = \mathrm{b}(\Omega_3^2 - \Omega_1^2) \quad (32)$$

$$u_4 = \mathrm{d}(\Omega_4^2 + \Omega_2^2 - \Omega_3^2 - \Omega_1^2) \quad (33)$$

Ω is the angular velocity of each rotor and Ω_d is expressed as follows:

$$\Omega_d = -\Omega_1 + \Omega_2 - \Omega_3 + \Omega_4 \quad (34)$$

III. Controller Design

A. *Strategy for Control of UAVs*

Linear Controllers: To work with the linearized model the linear control technique is first option to apply in model. The more effective controller for linearized model is PID controller that has easily implemented by hit and trail rule. By using PID controllers many scholars successfully implemented their models [12] and [14]. LQR is integrates with the PID controller for the satisfactory results [2]. H_∞ controller is applied for robust control on the linearized model.

Non-Linear Controllers: To address the limitations of linear control algorithms used in UAVs, many nonlinear flight controllers have been proposed. The nonlinear dynamic model is used to develop nonlinear control strategies.

Backstepping is a well-known repetitive approach for underactuated system control. This approach has a high rate of convergence and can manage external disturbances, but it is not robust. Fractional order controller is a reliable control that integrates with backstepping, radial basis functions and with the sliding mode controller. By using this scheme, the scholars can get the satisfactory simulation results [10]-[12].

Altitude is chosen to represent one translational dimension and yaw is chosen to represent one rotational dimension.

B. *Fractional Order Sliding Mode Controller*

Sliding Mode Controller: A kind of variable structure control (VSC) is sliding mode control (SMC). Traditionally, the closed-loop system's state space of the VSC consists of several structures at various locations. The isolated structures could be unstable, but by setting specific rules to transfer the control efforts among these structures, desirable performance is accomplished. Thus, regardless of the characteristics of the isolated structures, a closed-loop system with specific traits is produced.

The design of sliding mode design technique involves two phases. Designing a switching function is the first step in ensuring that the sliding motion complies with design requirements. SMC uses the switching control rule to accomplish two design goals. First, it moves the system's state trajectory onto the switching or sliding surface, a predetermined and user-selected surface in the state space. In logic, the surface is known as switching and depending on where in the state trajectory a state is, whether it is "above" or "below," the control path will have a different gain.

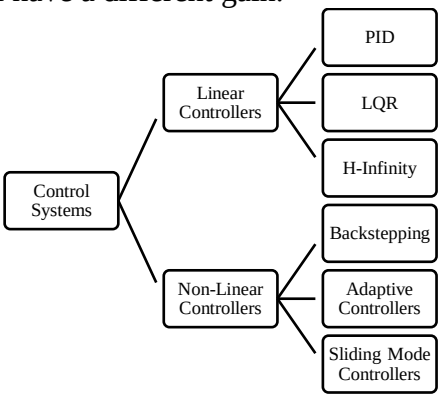

Fig. 4 Different Control Techniques for Quadcopter

The system's state trajectory on the switching surface is then maintained for the remainder of the time. The primary successes of the sliding mode design method are the ability to tailor the system's dynamic behavior through the selection of a specific switching function, and (ii) the system's closed-loop response becoming insensitive to known uncertainties. The design strategy is generally adequate for strong control given the latter benefit.

Sliding Surface Design: Consider the dynamical system below.

$$\dot{x} = Ax + bu, \qquad x \in \Re^n, \quad u \in \Re \tag{35}$$

Where A is square matrix of order *n*, *b* is an nth-order column vector, *x* represents the system state, *u* is the control input, and the controller receives n-dimensional input data $x \in \Re^n$. A sliding surface might be made to look like

$$s(x) = E^T x = \sum_{i=1}^{n} \sigma_i \, x_i = \sum_{i=1}^{n-1} \sigma_i \, x_i + x_n \tag{36}$$

Where *E* is sliding surface parameter vector given as $E = [\sigma_1 \quad ... \quad \sigma_{n-1}]^T$

C. *Yaw Control*

Yaw error is the difference of current yaw angle and desired yaw angle.

$$e_\psi = \psi - \psi_d \tag{37}$$

Taking double derivative on both sides

$$\ddot{e}_\psi = \ddot{\psi} - \ddot{\psi}_d \tag{38}$$

To cancel the effect of nonlinear terms and uncertainty choose appropriate u

$$u_4 = I_z\left(-a_5\dot{\phi}\dot{\theta} + \mu_\psi + \ddot{\psi}_d - k_\psi \dot{e}_\psi + u_1\right) \tag{39}$$

$$I_z\mu_\psi + u_1 = \dot{s}_\psi \tag{40}$$

We utilize the following Lyapunov functions to get an estimated level of uncertainty.

$$V_\psi = \frac{1}{2}s_\psi^2 + \frac{1}{2}\tilde{\varsigma}_\psi r_\psi \tilde{\varsigma}_\psi \tag{41}$$

$\tilde{\varsigma}_\psi$= Error between actual uncertainty and estimated uncertainty

r_ψ is a positive constant.

$\dot{\hat{\varsigma}}_\psi$= Estimated uncertainty

And,

$$u_1 = -\hat{\xi} - k_{1_\psi}\, sgn\left(s_\psi\right) - k_{2_\psi} s_\psi \tag{42}$$

The control gains must be as large as possible to ensure that the system behaves robustly against modeling uncertainties, but this leads to chattering, which causes many issues like vibrations in the mechanical structure of the quadrotor; as a result, reduces the chattering effect, control gains are estimated as follows.

$$k_{1_\psi} = \beta_\psi \left|s_\psi\right| \tag{41}$$

Where β_ψ is a positive constant.

D. *Altitude Control*

The dynamics of quadrotor's altitude are provided by,

$$\ddot{z} = -g + (cos\phi cos\theta)\frac{u_1}{m} \tag{42}$$

where

$$u_1 = b(\Omega_1^2 + \Omega_2^2 + \Omega_3^2 + \Omega_4^2) \tag{43}$$

Error is given by difference in desired and actual value of altitude

$$e_z = z - z_d \tag{44}$$

Taking derivative on both sides

$$\dot{e}_z = \dot{z} - \dot{z}_d \quad (45)$$

$$\ddot{e}_z = \ddot{z} - \ddot{z}_d \quad (46)$$

Sliding surface is assume as

$$s = \dot{e} + ke \quad (47)$$

Taking derivative on both sides

$$\dot{s} = \ddot{e} + k\dot{e} = \ddot{z} - \ddot{z}_d + k\dot{e} \quad (48)$$

Using the exponential reaching law

$$\dot{s} = -k_1 sgn(s) - k_2(s) \quad (49)$$

To cancel the effect of nonlinear terms control input is chosen as

$$u_1 = \frac{m}{(cos\phi cos\theta)}(g + \ddot{z}_d - k\dot{e} - k_1 sgn(s)) \quad (50)$$

Fractional order integral and derivative operators are represented by the symbol D_t^p. Their integral and derivative are given by the following equation,

$$D_t^p = \begin{cases} \frac{d^p}{dt^p} & \mathcal{R} > 0 \\ 1 & \mathcal{R} > 0 \\ \int_a^t dt^{-p} & \mathcal{R} > 0 \end{cases} \quad (51)$$

Caputo fractional method is defined as,

$$D_t^p f(t) = \frac{1}{\Gamma(n-p)} \int_a^t \frac{f^n(\tau)}{(t-\tau)^{p-n+1}} d\tau \quad (52)$$

Riemann-Liouville method is defined as,

$$D_t^p f(t) = \left(\frac{d}{dt}\right)^n \frac{1}{\Gamma(n-p)} \int_a^t \frac{f^n(\tau)}{(t-\tau)^{p-n+1}} d\tau \quad (53)$$

Γ is a gamma function states that in Equation 53, and $n-1 < p < n$,

$$\Gamma(p) = \int_0^\infty e^{-x}.x^{p-1}\, dx \quad (54)$$

The quadcopter altitude sliding surface can be re-defined using the derivative and integral of the fractional order:

$$s_{fh} = D_t^{1+\beta} e_h(t) + k_h e_h \quad (55)$$

A fractional order sliding surface for altitude control is represented by s_{fh} and k_h is a positive constant. Studying the sliding surface derivation can also change the altitude control signal in a FO. The Eq. 50 becomes,

$$u_1 = \frac{m}{(cos\phi cos\theta)}(g + \ddot{z}_d - kD_t^{1-\beta} - k_1 sgn(s)) \quad (56)$$

IV. Results and Discussion

In this section controllers are designed based on the discussion in Section III and applied to the quadcopter model.

Firstly, used the built in block of PD controller, and adjusting the gains by hit and trail method [32]. Then applied the proposed controller and compare the results of both controllers.

A. *Step Input without Disturbance*

Figure 5 shows the PD controller's yaw reaction, the parameters proportional and derivative values are 0.004 and 0.0012. Table 2 provides a summary of that data. The response has a 25% overshoot at 0.48 sec and a 1.21 s settling time when step input is used. The Red line indicates a response, whereas the blue line displays a command.

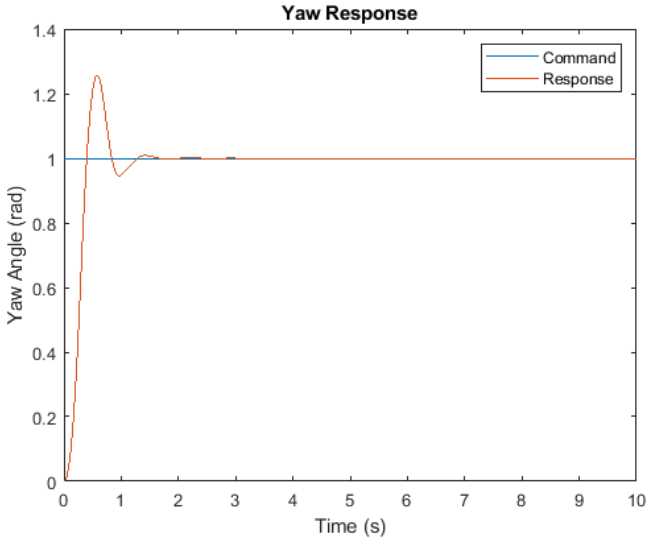

Fig. 5 Yaw Response of PD Controller

For the FO-SMC controller used, the yaw response is currently being examined. Figure 6 displays the outcomes, and Table 2 provides an overview of them. The overshoot has been effectively decreased to zero using fractional order SMC. The command is shown on the blue line, and the answer is shown on the red line. This occurred because of switching terms that tightly maintained the system's sliding surface.

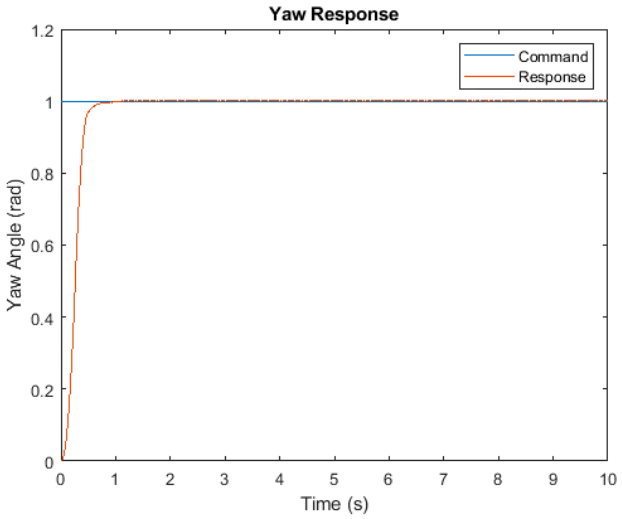

Fig. 6 Yaw Response of FO-SMC Controller

Table 2. Yaw Response of PD & FOSMC Controller

Description	PD	FOSMC
Rise Time	0.38 s	0.46 s
Percentage overshoot	25.7 %	Nil
Settling Time	1.21 s	0.56 s

Figure 7 and Table 3 provide the altitude response for the PD controller by adjusting the parameters PD are 0.8 and 0.3 respectively. The response to a 1 m step input exhibits a significant overrun of 62% at 1.3 s and a significant settling period of 2.6 s.

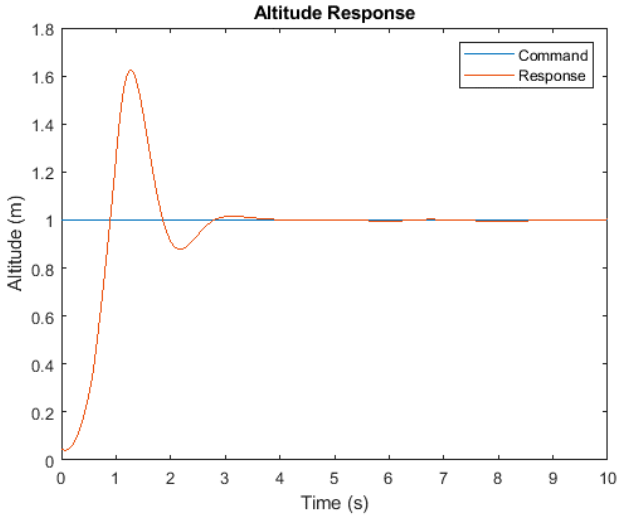

Fig. 7 Altitude Response of PD Controller

For the FO-SMC controller, the altitude response is currently being examined. Figure 8 displays the results, which are reported in Table 3. FOSMC has been able to successfully minimize the overshoot to just 29.22%. The rising time is 0.311 s, while the settling time is 1.4 s. This occurred because of switching terms that tightly maintained the system's sliding surface.

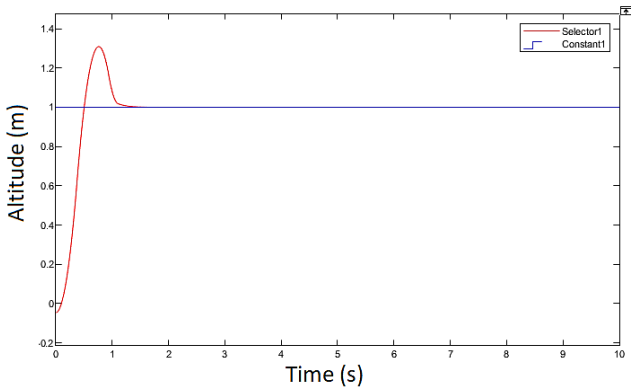

Fig. 8 Altitude Response of FO-SMC

Table 3. Results of Altitude Response of PD & FOSMC

Description	PD	SMC	FOSMC
Rise Time	0.87 s	1.06	0.311 s
Percentage overshoot	62 %	5.3%	29.22%
Settling Time	2.67 s	1.4 s	1.457 s

The figures clearly show that the FO-SMC has improved performance in terms of overshoot for yaw from 25% to 0%. For yaw, the settling time is lowered from 1.2 s to 0.5 s. The rising time for yaw has increased somewhat from 0.38 s to 0.46 s. Altitude overshoot was cut in half, from 62% to 29%. The settling time is lowered from 2.7 to 1.457 seconds. The rise time for altitude has reduced somewhat from 0.87 s to 0.311 s. Planning a flight path and formation is made much easier by this feature.

B. Chattering Attenuation

Figures 9 and 10 depict the chattering phenomenon rapid jumps in actuator command values between the maximum and minimum which causes vibrations and mechanical wear and tear.

Utilizing the saturation function as opposed to the sign function Figures 11 and 12 demonstrate how the chattering has been eliminated. There is no wind disruption in this scenario and a step input is used.

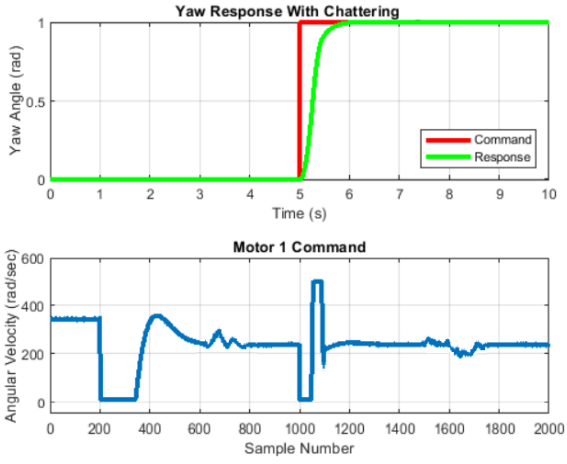

Fig. 9 Yaw Response with Chattering Simulation

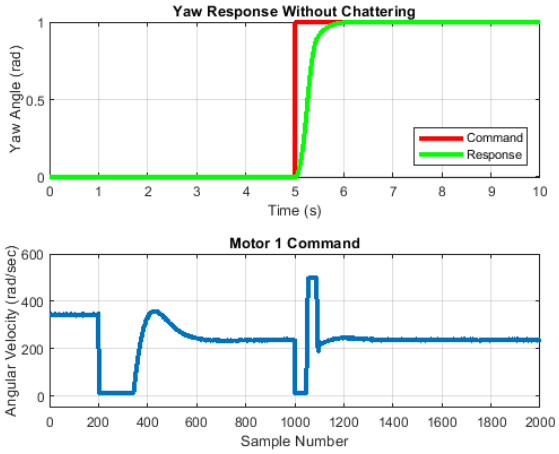

Fig. 10 Yaw Response without Chattering

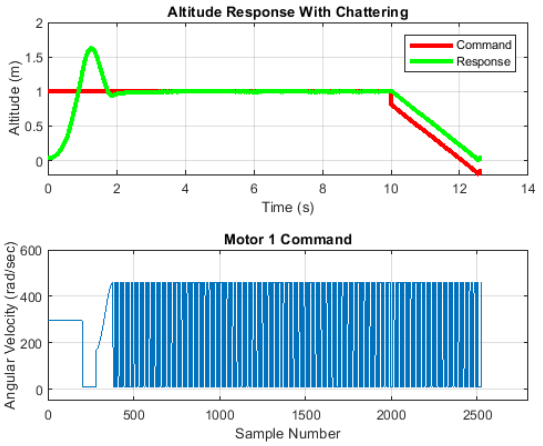

Fig. 11 Altitude Response with Chattering

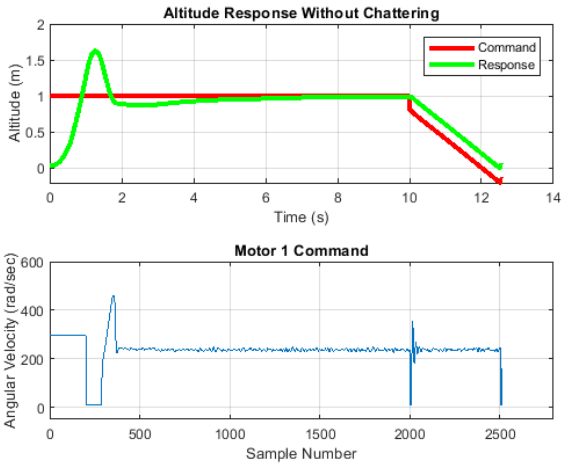

Fig. 12 Altitude Response without Chattering

C. *Wind Disturbance*

The introduction of wind disruption in the body frame's x and y axes. The effects of wind disturbance can cause variations in thrust and power, as well as roll, pitch, and yaw, which can make the flight more challenging. In Figure 13, the results of the PD and FO-SMC controller are displayed. For yaw, a step input of 1 radian is used. The sinusoidal wind disturbance cannot be rejected by the PD when it occurs. In the instance of the FO-SMC controller, wind disturbance in the body frame's x and y axes are not creating any divergence from the mandated value.

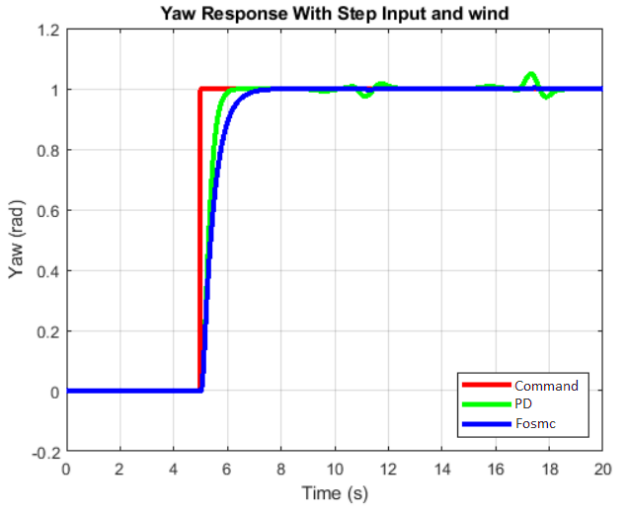

Fig. 13 Yaw Response of FO-SMC and PD Controller with Wind and Step Input

To evaluate the effectiveness of the altitude controller, wind disturbance was induced into the body frame's z-axis.

In the case of the FO-SMC controller for step, as illustrated in Figure 14, wind disturbance in the body frame z-axis is creating a minor deviation from the required value.

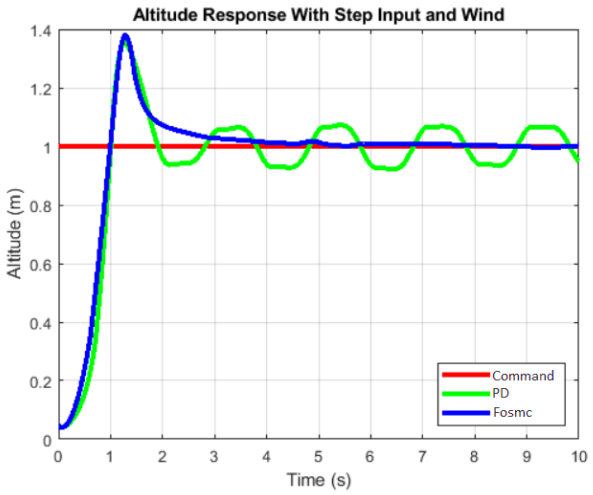

Fig. 14 Altitude Response with Step Input and Wind

V. Conclusion and Future Work

In this study, the rising time, settling time, and percentage overshoot in simulations for PD and FO-SMC are compared. With a little increase in rise time, the FO-SMC has enhanced performance in terms of overshoot and settling time. Planning a flight path and formation can be made much easier by this feature. Also offered is a comparison between fractional order sliding mode and PD under wind disturbances in simulations. While the FO-SMC entirely rejects wind disturbances, the PD controller is unable to do so. On hardware with wind disturbance, FO-SMC is used with positive outcomes.

It is advised that several control settings be tuned in future research. For this, a suitable optimization method must be created and used. The use of fractional order sliding mode on various UAV designs is another consideration. A smooth reaching phase may also be achieved by using a higher order sliding mode.

References

[1] S. Bouabdallah, A. Noth, and R. Siegwart, "PID vs LQ control techniques applied to an indoor micro quadcopter", 2004 IEEE/RSJ International Conference on Intelligent Robots and Systems (IROS), Sendai, Japan, 2004, vol. 3, pp. 2451-2456.

[2] C. Nicol, C.J.B. Macnab, and A. R. Serrano, "Robust adaptive control of a quadcopter helicopter", Mechatronics, vol. 21, no. 6, pp. 927-938, 2011.

[3] B. Sumantri, N. Uchiyama, S. Sano, and Y. Kawabata, "Robust tracking control of a Quad-Rotor helicopter utilizing sliding mode control with a nonlinear sliding surface", Journal of System Design and Dynamics, vol. 7, no. 2, pp. 226-241, 2013.

[4] M. Fatan, B. L. Sefidgari, and A. V. Barenji, "An adaptive neuro pid for controlling the altitude of quadcopter robot", in 2013 18th International Conference on Methods & Models in Automation & Robotics (MMAR), Miedzyzdroje, Poland, 2013, pp. 662-665.

[5] A. Razinkova, I. Gaponov, and H. C. Cho, "Adaptive control over quadcopter UAV under disturbances", in 2014 14th International Conference on Control, Automation and systems (ICCAS 2014), Gyeonggi-do, Korea (South), 2014, pp. 386-390.

[6] E.G. Hernandez, G. F. Fernandez, E. D. Ferreira, J. J. Flores, and A. Lopez, "Trajectory tracking of a quadcopter UAV with optimal translational control", Journal of IFAC-PapersOnline, vol. 48, no. 19, pp. 226-231, 2015.

[7] F. Santoso, M. A. Garrat, and G. Anavatti, "Fuzzy logic-based tuning autopilots for trajectory tracking of a low-cost quadcopter: A comparative study", in 2015 International Conference on Advanced Mechatronics, Intelligent Manufacture, and Industrial Automation (ICAMIMIA), Surabaya, Indonesia, 2015, pp. 64-69.

[8] F. Chen, F. Lu, B. Jiang, and G. Tao, "Adaptive compensation control of the quadcopter helicopter using quantum information technology and disturbance observer", Journal of the Franklin Institute, vol. 351, no. 1, pp. 442-455, 2014.

[9] F. Chen, F. Lu, B. Jiang and G. Tao, "A Reconfiguration Scheme for Quadcopter Helicopter via Simple Adaptive Control and Quantum Logic", IEEE Transactions on Industrial Electronics, vol. 62, no. 7, pp. 4328-4335, 2015.

[10] C. Ha, Z. Zuo, F. B. Choi, and D. Lee, "Passivity-based adaptive backstepping control of quadrotor-type UAVs", Robotics and Autonomous Systems, vol. 62, no. 9, pp. 1305-1315, 2014.

[11] C. Peng, Y. Bai, X. Gong, Q. Gao, C. Zhao, and Y. Tian, "Modeling ad Robust Backstepping Sliding Mode Control with Adaptive RBFNN for a Novel Coaxial Eight-rotor UAV", IEEE/CAA Journal of Automatic Sinica, vol. 2, no. 1, pp. 56-64, 2015.

[12] S. J. Haddadi, P. Zarafshan, and F. J. Niroumand "Dynamics Modelling and Implementation of an Attitude Control on an Octorotor", in Proceeding of the 2015 IEEE 28th, Canadian Conference on Electrical and Computer Engineering (CCECE), Halifax, Canada, 2015, pp. 722-727.

[13] M. Saied, B. Lussier, I. Fantoni, C. Francis, H. Sharim, and G. Sanahuja, "Fault diagnosis and fault-tolerant control strategy for rotor failure in an octorotor", in Proceeding of the 2015 IEEE International Conference on Robotics and Automation (ICRA), Seattle, WA, USA, 2015, pp. 5266-5271.

[14] S. Islam, M. Faraz, R. K. Ashour, G. Cai, J. Dias, and L. Seneviratne "Adaptive sliding mode control design for quadrotor unmanned aerial vehicle", in Proceeding of the 2015 International Conference on Unmanned Aircraft Systems (ICUAS), Denver, CO, USA, 2015, pp. 34-39.

[15] M. Saied, H. Shraim, C. Francis, I. Fantoni, B. Lussier, "Actuator fault diagnosis in an octorotor UAV using sliding modes techniques: Theory and experimentation",

in Proceeding of 2015 European Control Conference, Linz, Austria, 2015, pp. 1639-1644.
[16] M. Saied, B. Lussier, I. Fantoni, C. Francis, and H. Sharim, "Fault tolerant control for multiple successive failures in an octorotor: Architecture and experiments", in Proceeding of 2015 IEEE/RSG International Conference on Intelligent Robots and Systems (IROS), Hamburg, Germany, 2015, pp. 40-45.
[17] R. U. Amin and A. Li, "Modelling and robust attitude trajectory tracking control of 3-DOF four rotor hover vehicle", Aircraft Engineering and Aerospace Technology, pp. 2017.
[18] R. U. Amin and A. Li, "Design of mixed sensitivity H∞ control for four-rotor hover vehicle", International Journal of Automation and Control, vol. 11, no. 1, pp. 89-103, 2017.
[19] S. Zeghlache, H. Mekki, A. Bouguerra, and A. Djerioui, "Actuator fault tolerant control control using adaptive RBFNN fuzzy sliding mode controller for coaxial octorotor UAV", ISA Transaction, vol. 80, pp. 267-278, 2018.
[20] J. Velagic, N. Osmic, B. Puscul, and S. Krilasevic, "Identification, Model Validation and Control of an Octorotor Unmanned Aerial Vehicle", in Proceeding of 2018 IEEE International Conference on Industrial Informatics (INDIN), Porto, Portugal, 2018, pp. 381-387.
[21] S. Bari, S. S. Z. Hamdani, H. U. Khan, M. Rehman, and H. Khan, "Artificial Neural Network Based Self-Tuned PID Controller for Flight Control of Quadcopter", in Proceeding of 2019 International Conference on Engineering and Emerging Technologies (ICEET), Lahore, Pakistan, 2019, pp. 1-5.
[22] N. Yan, C. Wang, Y. Tao, J. Li, K. Zhang, T. Chen, X. Yan, and G. Wang, "Quadcopter Control System Using a Hybrid BCI Based on Off-Line Optimization and Enhanced Human Machine Interaction", IEEE Access, vol. 8, pp. 1160-1172, 2019.
[23] R. U. Amin, I. Inayat, and L. A. Jun, "Finite time position and heading tracking control of coaxial octorotor based on extended inverse multi-quadratic radial basis function network and external disturbance observer", Journal of the Franklin Institute, vol. 356, no. 8, pp. 4240-4269, 2019.
[24] D. Soberl, I. Bratko, and J. Zabkar, "Learning to Control a Quadcopter Qualitatively", Journal of Intelligent & Robotic Systems, vol. 100, no. 3, pp. 1097-1110, 2020.
[25] M. Al-Fetyani and A. Alsharkawi, "Design of an Executable ANFIS-based Control System to Improve the Attitude and Altitude Performances of a Quadcopter Drone", International Journal of Automation and Computing, vol. 18, no. 1, pp. 124-140, 2021.
[26] S. I. Abdelmaksoud, M. Mailah, and A. M. Abdallah, "Improving Disturbance Rejection Capability for a Quadcopter UAV System Using Self-Regulating Fuzzy PID Controller", 2020 International Conference on Computer, Control, Electrical, and Electronics Engineering (ICCCEEE), Khartoum, Sudan, 2021, pp. 1-6.
[27] S. Ullah, Q. Khan, A. Mehmood, S. Rehman, and J. Iqbal "Robust Integral Sliding Mode Control Design for Stability Enhancement of Under-actuated Quadcopter", International Journal of Control, Automation and Systems, vol. 18, pp. 1671-1678, 2020.
[28] S. Ullah, Q. Khan, A. Mehmood, S. A. M. Kirmani, and O. Mechali, "Neuro-adaptive fast integral terminal sliding mode control design with variable gain robust exact differentiator for under-actuated quadcopter UAV", ISA Transactions, vol. 120, pp. 293-304, 2022.
[29] Riether, Fabian, "Agile Quadcopter Maneuvering using Tensor-Decomposition-based globally optimal control and onboard visual-inertial Estimation", Massachusetts Institute of Technology, 2016.
[30] A. Eltayeb, M. F. Rahmat, M. A. M. Basri, M. A. M. Eltoum, and S. El-Ferik, "An Improved Design of an Adaptive Sliding Mode Controller for Chattering Attenuation and Trajectory Tracking of the Quadcopter UAV", IEEE Access, vol. 8, pp. 205968-205979, 2020.
[31] O. N Gasparyan and H. G Darbinyan, "Adaptive System of Compensation of Motors Partian Degradations of Multirotor UAVs", Modern Problems of Robotics: Second International Conference, MPoR 2020, Moscow, Russia, 2021, pp. 207-219.
[32] Quadcopter Project, MathWorks, available online at https://www.mathworks.com/help/aeroblks/quadcopter-project.html, Accessed 8 April 2022.